Supplemental Material

Supplemental text

Text S1: Photobleaching

In two previous reports of the quantification of molecules in fluorescent foci in bacteria by step-wise photobleaching, total internal reflection fluorescence (TIRF) microscopy was used (1, 2). We attempted this method with the Nikon Eclipse Ti inverted microscope (Nikon Instruments) in TIRF mode using a 100X 1.49 NA TIRF objective, and Argon/AOTF 514 nm laser illumination at 20% power setting using TIRF filter cube (TIRF 488-561-640) and YFPHQ emission filter. Although the intensity and wavelength of the laser gave very good signals, we found that the results were inconsistent. Specifically, the intensity drop attributable to the bleaching of a single molecule varied over 8-fold among foci. Although results with such high magnitudes of variation have been used to calculate stoichiometry of fluorescent foci (1, 2), we sought to find a more precise method for our experiments. Since with TIRF microscopy only a thin area between the specimen and the microscope slide is illuminated, the intensity of individual foci will vary with their position in the field. In addition, the number of free fluorescent DinB molecules in the cell is high, exceeding the number that are localized in foci; since the free molecules can drift in and out of the photobleaching area, they contribute a high and variable background fluorescence. To eliminate these problems we performed the photobleaching experiments with the microscope in epifluorescent mode.

Text S2: Tagged Pol IV constructs that are inactive or not useful. In attempts to create a fully active Pol IV protein that we could localize microscopically we made several other tagged DinB constructs. To use FLASH technology (3) we fused a tetracystein (TC) tag to the N-terminus of DinB. A fusion we used previously, STREP-FLAG Pol IV, is fully active for adaptive mutation when expressed from a high-copy vector (4). Building on this, we also fused a TC-STREP-FLAG tag to the N-terminus of DinB. Both of these fusions complemented the NQO-sensitive phenotype of a Δ*dinB* mutant strain but were inactive for adaptive mutation (data not shown). We also fused the 3X-FLAG peptide to the N-terminus of DinB; this fusion complemented the NQO-sensitive phenotype of a Δ*dinB* mutant strain and retained partial (70%) adaptive mutation activity. But in attempts to localize the 3X-FLAG tagged Pol IV by immunofluorescence microscopy we were unable to obtain specific staining and reproducible results with anti FLAG primary Ab and a fluorescent secondary antibody (data not shown).

Text S3: Distance between the I-*Sce*I recognition site and the *lacO* array has little effect on the fraction of Pol IV foci that are coincident with instead of adjacent to LacI foci. In our first strain constructions the distance between the *lacO* array and the I-SceI site was 161 Kb. In co-localization experiments with these strains not all Pol IV and LacI foci were coincident, but a variable fraction were adjacent (0.2-0.5 μm apart). An explanation for this result is that Pol IV localizes to the DSB and then moves away as it replicates the DNA. However, in a previous study involving labeling DSB sites with arrays such results were found to depend on the distance between DSB site and *lacO* array (5). To test this hypothesis in our experiments, we constructed strains with the I-*Sce*I recognition site closer to the *lacO* array.

The I-*Sce*I recognition site was inserted by recombineering (6) into the *thrS-arpB'* intergenic region at 1.801 Mb, 2.2 Kb from the *lacO* array. Plasmid pPFV427 was used as template to amplify FRT-*cat*-FRT-I-*Sce*I cassette with primers "5' Homo thrS-arpB Wanner P1" and "3'Homo thrS-arpB Wanner P4" (Table 2). The PCR product was recombineered into strain FC36 as described in the Materials and Methods, creating strain PFB1248 with FRT-*cat*-FRT-I-*Sce*I at 1.801 Mb. $P1_{vir}$ transduction was used to transfer this allele into PFB1041 (FC36::*lacZo*::Kn), selecting for Cm^R, Kn^R transductants. The Cm^R gene was removed using Flp recombinase and insertion of the I-*Sce*I recognition site was confirmed by sequencing. To confirm the functionality of the I-*Sce*I recognition site, primers "5' thrS-arpB US Fwd" and "3' thrS-arpB DS Rev" (Table 2) were used to amplify I-*Sce*I site insertion region flanked by 150 bp upstream and downstream sequences, and the PCR product digested with recombinant I-*Sce*I endonuclease.

Comparisons of the results with the strains carrying the I-*Sce*I recognition site and the *lacO* array separated by the two distances are given in Table S2. With the exception of the result with the wild-type strain, which appears to be an outlier, the proportion of coincident foci when the *lacO* array and the I-SceI recognition site were closer increased from about 70% to about 80%. Thus, the distance between the LacI foci and the DSB had only a marginal effect on the co-localization of Pol IV with LacI.

Table S1: Parameters of the step-wise photobleaching analysis

Trace	μ	Delta	Unitary step Size	Initial ROI-Focus	Initial ROI-Cyto	I Focus	Number of Molecules
1	3	3324	1108	4466	2113	2353	2.12
2	4	4633	1158	6182	2981	3202	2.76
3	4	3622	905	5789	4106	1682	1.86
4	3	4263	1421	6425	4222	2202	1.55
5	2	1477	738	5879	2113	3766	5.10
6	4	2770	693	5300	3346	1954	2.82
7	4	2799	700	4459	2344	2115	3.02
8	5	4672	934	9416	3492	5924	6.34
9	3	2579	860	7640	3492	4148	4.83
10	4	5822	1456	9886	3030	6856	4.71
11	7	5609	801	7702	5439	2263	2.82
12	4	4420	1105	5789	4106	1683	1.52
13	6	3732	622	5225	3983	1242	2.00
14	4	4557	1139	6183	2981	3201	2.81
15	4	4420	1105	5790	4107	1683	1.52
16	3	3654	1218	6425	4222	2202	1.81
17	3	2966	989	5296	2008	3289	3.33
18	4	3781	945	9416	3492	5924	6.27
19	3	3618	1206	6058	3492	2566	2.13
20	4	5159	1290	10514	2155	8359	6.48
21	4	4477	1119	7217	1652	5565	4.97
22	3	3610	1203	7725	1742	5984	4.97
23	3	4389	1463	8624	2324	6300	4.31
24	4	4623	1156	10770	3483	7288	6.31
25	4	6236	1559	13959	3842	10117	6.49
26	5	7214	1443	12677	3454	9222	6.39
27	5	7445	1489	9494	3464	6030	4.05
28	4	5413	1353	11255	3128	8127	6.01
29	4	3305	826	6157	2439	3718	4.50
30	3	3335	1112	7312	1316	5996	5.39
31	3	2594	865	7302	2044	3963	4.58
32	4	1928	482	2907	1444	1463	3.04
33	4	5608	1402	8007	3962	4045	2.89
34	5	5035	1007	8468	2882	5586	5.55
35	2	1603	801	5206	2693	2514	3.14
36	3	2517	839	3818	1601	2217	2.64
37	2	2718	1359	6285	4315	1970	1.45
38	3	3256	1085	5798	2638	3160	2.91
39	3	4083	1361	9988	1908	8080	5.94
40	3	3631	1210	5605	1411	4195	3.47
41	2	2048	1024	3347	952	2394	2.34
42	2	1711	856	4531	1486	3045	3.56
43	5	4236	847	6029	1338	4691	5.54
44	3	2562	854	4585	1869	2716	3.18
45	4	5212	1303	7607	1444	6163	4.73
mean	3.67	3926	1076	7078	2801	4248	3.87
SD	1.04	1397	263	2428	1064	2325	1.62

min	2	1477	482	2907	952	1242	1.45
max	7	7445	1559	13959	5439	10117	6.49
max/min	3.5	5.04	3.23	4.80	3.50	8.14	4.48

Trace = photobleaching trace number; μ = the number of peaks in the PDDF-histogram as given by the dominant peak of the Fourier transform of the PDDF histogram bin values; Delta = the maximum PDDF value = the difference between the maximum and minimum values of the fitted Chung Kennedy step-curve; Unitary step Size = delta/ μ; Initial ROI-focus = the initial intensity of the region of interest that included a Pol IV focus; Initial ROI-cyto = the initial intensity of a nearby region of interest that did not include the Pol IV focus; I-focus = initial intensity of the focus = (Initial ROI-focus)-(Initial ROI-cyto); number of molecules = I-focus/unitary step size. SD = standard deviation; min = minimum value; max = maximum value.

Table S2: The effect of the distance between the I-SceI site and the *lacO* array on co-localization of LacI and Pol IV foci

Distance between I-SceI site and *lacZ*o	Strain	DinB Fusion	% of foci co-localized	% of the co-localized foci	
				Coincident	Adjacent
161 Kb	*WT	DinB-12L-EYFP	62 ± 13	27 ± 4	73 ± 4
	*Δ*dinB*	DinB-12L-EYFP	81 ± 20	63 ± 5	37 ± 5
	*Δ*umuDC*	DinB-20L-EYFP	63 ± 8	63 ± 5	37 ± 1
	*Δ*dinB* Δ*umuDC*	DinB-20L-EYFP	50 ± 10	80 ± 4	20 ± 4
2.2 Kb	†Δ*dinB*	DinB-20L-EYFP	47 ± 12	75 ± 4	25 ± 4
	†Δ*dinB* Δ*umuDC*	DinB-20L-EYFP	50 ± 10	84 ± 15	16 ±1 6
2.2 Kb	‡Δ*dinB*	DinB-20L-EYFP	30 ± 7%	86 ± 2	14 ± 2
	‡Δ*dinB* Δ*umuDC*	DinB-20L-EYFP	43 ± 6%	69 ± 5	31 ± 5

* Means ± SEMs for filamenting cells for the experiment shown in Fig. 6. The same percentages for Coincident and Adjacent given for the Δ*dinB* and Δ*umuDC* strains are not mistakes.
† Δ*dinB* = PFB1271 carrying plasmids pPFB1035 and pPFB1188; data are from three independent experiments; cells observed =152,149, and 168, respectively. Δ*dinB* Δ*umuDC* = PFB1279 carrying plasmids pPFB1035 and pPFB1188; data are from two independent experiments; cells observed = 233 and 161, respectively.
‡ Means ± SEMs for the experiment shown in Fig 7. These are non-filamenting stationary-phase cells.

Supplemental Figures

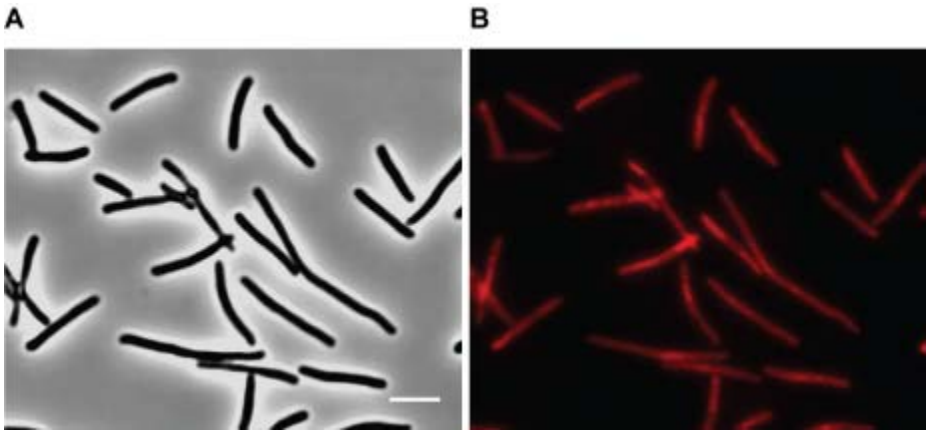

Figure S1: Rep does not form foci in the absence of Pol IV. Phase contrast (A) and fluorescent images (B) of a Δ*dinB* mutant strain carrying Rep-mCh after exposure to Nal. Strain PFB243 carrying pPFB914 was grown in LB broth plus antibiotics at 37°C to mid-exponential phase (OD_{600}= 0.5), treated or not with 40 μg/ml Nal, incubated for an additional 2 hr, and then visualized for mCh fluorescence. 10 Rep foci were observed in 4184 unexposed cells; of the Nal-exposed cells, >99% were filamenting and 3 Rep foci were observed in 1662 of these. Scale bar = 5μm.

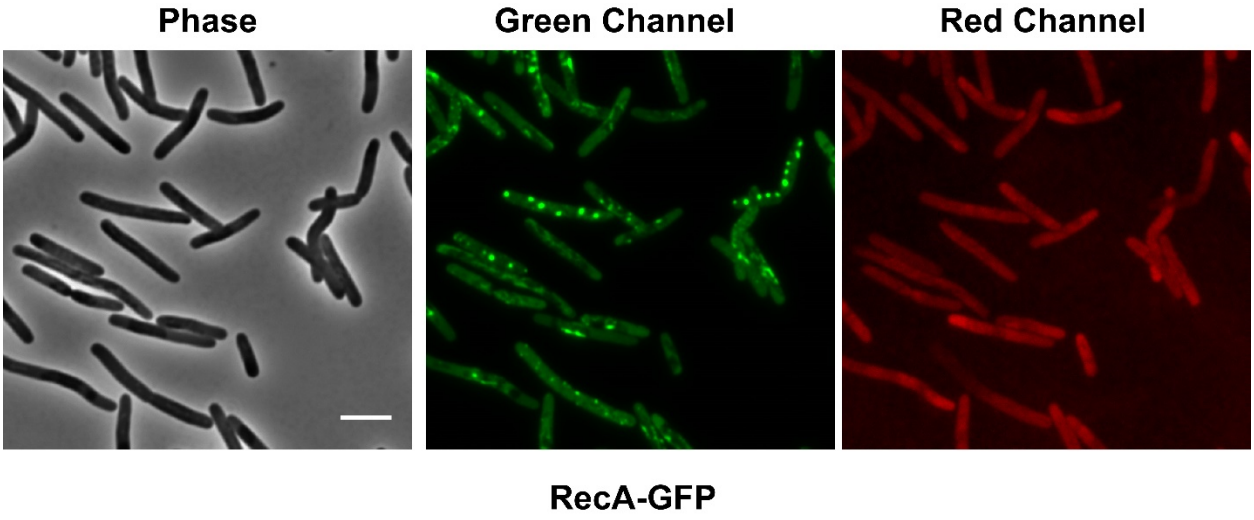

Figure S2: RecA-GFP does not bleed-through to the red channel. Phase contrast and fluorescent images of RecA-GFP foci formation after Nal exposure. Scale bar = 5 μm. Strain PFB1137 (=RecA-GFP) was grown in LB broth plus antibiotics at 30°C to mid-exponential phase (OD_{600}= 0.5), treated with 40 μg/ml Nal, incubated for an additional 45 min, and then visualized. RecA-GFP foci were visualized in the green channel using a C-FL HYQ FITC filter cube; the same image was visualized in the red channel using the C-FL HYQ Texas Red Filter Cube that is used for mCherry fusions. The brightness of the red image has been enhanced to show that no RecA-GFP foci appear. Scale bar = 5μm.

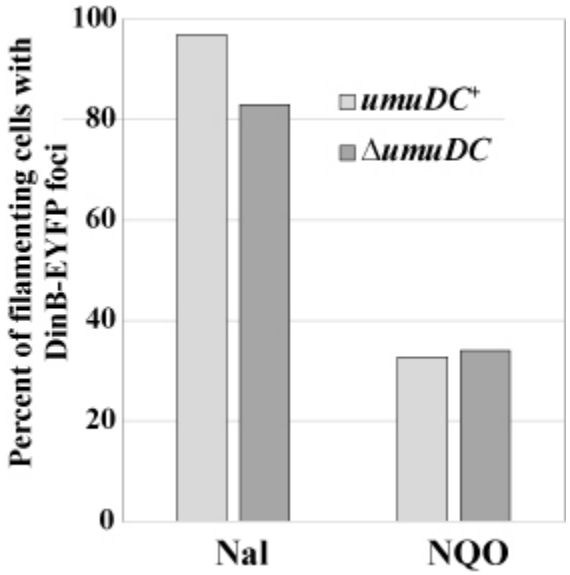

Figure S3: Pol V does not interfere with Pol IV foci formation after DNA damage. The Δ*dinB umuDC*$^{+}$ strain PFB236 and Δ*dinB* Δ*umuDC* strain PFB1263, each carrying DinB-12L-EYFP (=pPFB913) were grown in LB broth plus antibiotics at 37°C to mid-exponential phase (OD_{600}= 0.5), treated with 40 μg/ml Nal or 160 μM NQO, and incubation continued. Shown are the percent of filamenting (SOS-induced) cells that contained Pol IV-EYFP loci 2 hrs after the addition of Nal, and 3 hrs and 20 min after the addition of NQO (cells examined: PFB236/pPFB913, Nal = 297 total, 297 filamenting, NQO = 1356 total, 308 filamenting; PFb1263/pB913, Nal = 790 total, 790 filamenting; NQO = 493 total, 258 filamenting). The results with NQO were weaker and more variable than with Nal, but it is clear that Pol V had little impact of foci formation by Pol IV.

REFERENCES

1. **Leake MC, Chandler JH, Wadhams GH, Bai F, Berry RM, Armitage JP.** 2006. Stoichiometry and turnover in single, functioning membrane protein complexes. Nature **443:**355-358.
2. **Lenn T, Gkekas CN, Bernard L, Engl C, Jovanovic G, Buck M, Ying L.** 2011. Measuring the stoichiometry of functional PspA complexes in living bacterial cells by single molecule photobleaching. Chem Commun (Camb) **47:**400-402.
3. **Griffin BA, Adams SR, Tsien RY.** 1998. Specific covalent labeling of recombinant protein molecules inside live cells. Science **281:**269-272.
4. **Sladewski TE, Hetrick KM, Foster PL.** 2011. *Escherichia coli* Rep DNA helicase and error-prone DNA polymerase IV interact physically and functionally. Mol Microbiol **80:**524-541.
5. **Shee C, Cox BD, Gu F, Luengas EM, Joshi MC, Chiu LY, Magnan D, Halliday JA, Frisch RL, Gibson JL, Nehring RB, Do HG, Hernandez M, Li L, Herman C, Hastings P, Bates D, Harris RS, Miller KM, Rosenberg SM.** 2013. Engineered proteins detect spontaneous DNA breakage in human and bacterial cells. Elife **2:**e01222.
6. **Datsenko KA, Wanner BL.** 2000. One-step inactivation of chromosomal genes in *Escherichia coli* K-12 using PCR products. Proc Natl Acad Sci U S A **97:**6640-6645.